Domain-Integral Analysis of Channel Waveguides in Anisotropic Multi-layered Media

Harrie J. M. Bastiaansen, Nico H. G. Baken, and Hans Blok

Abstract—**A domain-integral equation method is presented to determine both propagation constants and the electromagnetic field distributions of guided surface wave modes in integrated optical waveguides. Both the waveguide and its multi-layered embedding are anisotropic. The permittivity tensor of the embedding is assumed to be piecewise homogeneous. The kernels of the domain-integral equations consist of Green's tensors. The scattering-matrix formalism is used to construct the Green's tensors. The integral equations form an eigenvalue problem, where the electric field strength represents the eigenvector. This problem is solved numerically by applying the method of moments. Numerical results are presented for an anisotropic ridge waveguide, embedded in an anisotropic multilayered medium.**

I. Introduction

THE DEVELOPMENT of integrated optical devices creates a growing need for accurate mathematical models to analyse their waveguiding properties. For tight design criteria and a profound insight in the working of these devices, approximate methods often lack the necessary accuracy. Examples of such approximate methods are the (corrected) effective index method [1], [2], the semi-vectorial finite difference method [3], [4], and the scalar finite element method [5].

The treatment of the infinite transversal cross-section poses a major problem in the analysis of open waveguides using finite difference and finite element techniques. This problem can be approached either by imposing an artificial zero boundary condition [6], or by employing elements extending to infinity [7]. The first approach has the disadvantage of requiring an extensive computational domain, especially for calculating propagation constants near cut-off. The infinite elements have the disadvantage of unknown field-behavior of the infinite elements a priori. Therefore, the development of rigorous mathematical methods, allowing the computational domain to be restricted to the finite cross-section of the waveguide, is desirable.

Several of these methods, have been proposed. Goell [8], has developed the method of circular harmonic expansion, in which the interior and exterior fields are expanded in (modified) Bessel functions with unknown coefficients, which are determined by matching the tangential field-components around the boundary of the waveguide. Several surface-integral equation methods have been proposed by [9], [10], and [11]. These relate the fields and their normal derivatives on the boundary of the waveguide. To take inhomogenities of the waveguide into account, a combination with the finite-element method has been proposed [12]. These rigorous methods have the drawback of not being applicable to waveguides embedded in multi-layered media. The domain-integral equation method however, can overcome this drawback [13]–[15].

In this method, the waveguide is regarded as a perturbation of its embedding, allowing an integral equation for the electric field strength within the waveguide to be derived. Cottis *et al.* [16] have demonstrated how the method can be used to determine propagation constants of guided surface wave modes in waveguides embedded in two-layered media, whereas Kolk *et al.* [17] treated multilayered media. However, the analyses of [16], [17] could only handle isotropic embeddings. Since electro-optical devices require anisotropic materials (e.g., Lithium Niobate) an extension of the method is in order.

In this paper, the domain-integral equation method is extended to multi-media configurations consisting of anisotropic materials. A scattering-matrix formalism, which is inherently stable, is introduced to calculate the Green's tensors, which form the kernels of the domain-integral equations. This formalism has the advantage of using considerably less CPU-time than the formalism described in [17], using recursive transmission and reflection functions. Both propagation constants and modal field-distributions of guided surface wave modes in an anisotropic waveguide, embedded in an anisotropic multi-layered medium, are numerically computed. The results are compared with the results for a corresponding isotropic waveguiding structure. This shows how neglecting the anisotropic character of the waveguiding structure can influence the propagation constants of guided surface wave modes.

II. Formulation of the Problem

The waveguide $\mathfrak{D}^w$ is embedded with one subdomain of a stratified embedding. This embedding consists of N subdomains $\mathfrak{D}^1, \mathfrak{D}^2, \cdots, \mathfrak{D}^N$ which have finite thick-

Manuscript received October 15, 1991; revised April 10, 1992.

H. J. M. Bastiaansen and N. H. G. Baken are with PTT Research Neher Laboratory, St Paulusstraat 4, P.O. Box 421, 2260 AK Leidschendam, The Netherlands.

H. Blok is with the Department of Electrical Engineering, Delft University of Technology, Mekelweg 4, P.O. Box 5031, 2600 GA Delft, The Netherlands.

IEEE Log Number 9202136.

nesses $h^1, h_2, \cdots, h^N$ and are sandwiched between the semi-infinite substrate $\mathfrak{D}^0$ and the semi-infinite superstrate $\mathfrak{D}^{N+1}$. The position in space is specified using a right-handed Cartesian reference frame $Oxyz$; the x-axis is taken perpendicular to the interfaces of the subdomains. The z-axis is chosen such that the material properties of the waveguiding configuration are invariant in the z-direction. The origin O is situated in the center of the subdomain $\mathfrak{D}^k$, containing the waveguide $\mathfrak{D}^w$. A cross section perpendicular to the z-axis is given in Fig. 1. All subdomains of the embedding are assumed to be homogeneous and possibly anisotropic; thus, the permittivity profile of the embedding can be described with the stepwise-constant tensor $\underline{\underline{\epsilon}}^b(x)$. In this paper we restrict ourselves to a homogeneous permittivity tensor of the waveguide $\underline{\underline{\epsilon}}^w$, although the theory can be readily extended to waveguides being inhomogeneous [17]. Furthermore, only permittivity tensors (uniaxial or biaxial) are considered with principal axes coinciding with the base vectors (for a more elaborate analysis, see [18]). The components ϵ_{mn} of these permittivity tensors are equal to 0 for $m \neq n$, $(m, n = 1, 2, 3)$. The nonzero diagonal-components ϵ_{mm} will from now on be denoted as ϵ_m.

Time-harmonic solutions of the source-free Maxwell's equations are sought that represent guided surface wave modes propagating in the positive z-direction. The electromagnetic field constituents of angular frequency ω and axial wavenumber k_z have the form

$$\{\underline{E}, \underline{H}\}(x, y, z) = \{\underline{\tilde{E}}, \underline{\tilde{H}}\}(x, y; k_z) \exp(-jk_z z). \quad (1)$$

The complex time factor $\exp(j\omega t)$ is omitted throughout this paper. The waveguide $\mathfrak{D}^w$ being regarded as a perturbation of the embedding, the electric field $\underline{\tilde{E}}$ and the magnetic field $\underline{\tilde{H}}$ satisfy Maxwell's equations:

$$-\underline{\nabla}_t \times \underline{\tilde{H}}(x, y; k_z) + j\omega \underline{\underline{\epsilon}}^b(x) \underline{\tilde{E}}(x, y; k_z) = -\underline{\tilde{J}}^c(x, y; k_z),$$

$$\underline{\nabla}_t \times \underline{\tilde{E}}(x, y; k_z) + j\omega\mu_0 \underline{\tilde{H}}(x, y; k_z) = \underline{0}, \quad (2)$$

where $\underline{\nabla}_t = (\partial/\partial x, \partial/\partial y, -jk_z)$ and $\tilde{J}^c$ represents the electric constrast-source current density, that is defined within the waveguide $\mathfrak{D}^w$ through

$$\underline{\tilde{J}}^c(x, y; k_z) = j\omega\{\underline{\underline{\epsilon}}^w - \underline{\underline{\epsilon}}^b(x)\} \cdot \underline{\tilde{E}}(x, y; k_z) \quad (3)$$

and vanishes everywhere outside $\mathfrak{D}^w$.

Using Lorentz's reciprocity theorem, integral representations for the electric field and the magnetic field can be derived:

$$\underline{\tilde{E}}(x, y; k_z) = \iint_{\mathfrak{D}^w} \underline{\underline{\tilde{G}}}^{EE}(x, y; x', y'; k_z) \cdot \underline{\tilde{J}}^c(x', y'; k_z)\, dx'\, dy', \quad (4)$$

$$\underline{\tilde{H}}(x, y; k_z) = \iint_{\mathfrak{D}^w} \underline{\underline{\tilde{G}}}^{ME}(x, y; x', y'; k_z) \cdot \underline{\tilde{J}}^c(x', y'; k_z)\, dx'\, dy', \quad (5)$$

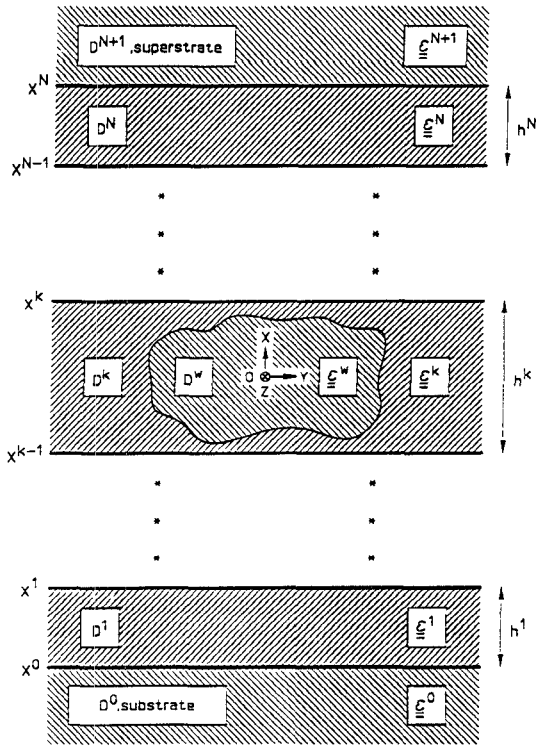

Fig. 1. Cross-section of the channel waveguide structure.

with $\underline{\underline{\tilde{G}}}^{EE}$ and $\underline{\underline{\tilde{G}}}^{ME}$ being the dyadic electric and magnetic Green's tensor, respectively. These Green's tensors are the solution of the inhomogeneous Maxwell equations:

$$-\underline{\nabla}' \times \underline{\underline{\tilde{G}}}^{ME}(x, y; x', y'; k_z) + j\omega \underline{\underline{\epsilon}}^b(x) \underline{\underline{\tilde{G}}}^{EE}(x, y; x', y'; k_z) = -\underline{\underline{I}} \cdot \delta(x - x', y - y'),$$

$$\underline{\nabla}_t \times \underline{\underline{\tilde{G}}}^{EE}(x, y; x', y'; k_z) + j\omega\mu_0 \underline{\underline{\tilde{G}}}^{ME}(x, y; x', y'; k_z) = \underline{0}, \quad (6)$$

with $\underline{\underline{I}}$ the unit tensor of rank 2 and $\delta(x, y)$ the two-dimensional Dirac delta function. Note that the relation in (4) expresses the electric field at an arbitrary point (x, y) in terms of the Green's tensor $\underline{\underline{\tilde{G}}}^{EE}$ and the electric field within the waveguide. If the point (x, y) is chosen within the waveguiding region $\mathfrak{D}^w$, (4) becomes a domain-integral equation for the electric field $\underline{\tilde{E}}$ within $\mathfrak{D}^w$. Solving this equation can be regarded as solving an eigenvalue problem. The equation yields nontrivial solutions for a discrete set of values k_z that corresponds to the propagation constants for propagating guided surface wave modes. Once these values have been determined, the corresponding electric field within $\mathfrak{D}^w$ can be computed. Subsequently, the electric field outside, and the magnetic field everywhere, can be evaluated from (4) and (5), respectively. To execute the procedure outlined in the foregoing, the kernel of the domain integral equations, the Green's tensors, must first be determined.

III. The Green's Tensors

The kernel of the domain-integral equations consists of the Green's tensors $\underline{\underline{\tilde{G}}}^{EE}$ and $\underline{\underline{\tilde{G}}}^{ME}$, which satisfy the inhomogeneous Maxwell equations (6). Instead of solving these equations for each of the columns of the unit tensor separately, we show how to solve

$$-\underline{\nabla}_t \times \underline{\tilde{H}}^G(x, y; x', y'; k_z) + j\omega \underline{\underline{\epsilon}}^b(x) \underline{\tilde{E}}^G(x, y; x', y'; k_z) = -\underline{\tilde{J}} \cdot \delta(x - x', y - y'), \quad (7)$$

$$\underline{\nabla}_t \times \underline{\tilde{E}}^G(x, y; x', y'; k_z) + j\omega\mu_0 \underline{\tilde{H}}^G(x, y; x', y'; k_z) = \underline{0}, \quad (8)$$

in which $\underline{\tilde{J}} = (\tilde{j}_1, \tilde{j}_2, \tilde{j}_3)$ is an arbitrary constant vector;

The ith column of the Green's tensor $\underline{\underline{\tilde{G}}}^{EE}$ ($\underline{\underline{\tilde{G}}}^{ME}$) equals the electric magnetic field $\underline{\tilde{E}}^G$ ($\underline{\tilde{H}}^G$), for $\underline{\tilde{J}}$ equal to the ith unit vector ($i = 1, 2, 3$). The superscript "^{G}" is used in order to avoid confusion between the electric and magnetic fields being solutions of the domain-integral equations (4), (5) and the electric and magnetic fields being solutions of the point-source problem (7), (8). The waveguide $\mathfrak{D}^w$ being completely embedded within subdomain $\mathfrak{D}^k$, the domain-integral equations (4), (5) can be solved when the Green's tensors (or equivalently, the solution of (7), (8)) are known for source points (x', y') and observation points (x, y) both situated inside this subdomain. The presence of the point source divides subdomain $\mathfrak{D}^k$ in two new subdomains $\mathfrak{D}^{k+}$ and $\mathfrak{D}^{k-}$, having thicknessess $h^{k+}$and h^{k-}, respectively (Fig. 2).

Several formalisms for solving Maxwell's equations (7), (8) are possible. A method using recurrence transmission and reflection functions for isotropic materials has been presented in [19]. A modified version of this formalism has been presented in [17]. In the present paper, a formalism, called the scattering-matrix formalism, is outlined.

Making use of the y-invariance of the embedding, Maxwell's equations (7), (8) are submitted to a spatial Fourier-transformation in the y-direction, defined as

$$\tilde{\tilde{f}}(k_y) = \int_{-\infty}^{\infty} \tilde{f}(y) \exp(jk_y y)\, dy,$$

$$\tilde{f}(y) = \frac{1}{2\pi} \int_{-\infty}^{\infty} \tilde{\tilde{f}}(k_y) = \exp(-jk_y y)\, dk_y, \quad (9)$$

yielding

$$-\underline{\nabla}_t \times \underline{\tilde{\tilde{H}}}^G(x; x', y'; k_y, k_z) + j\omega \underline{\underline{\epsilon}}^b(x) \underline{\tilde{\tilde{E}}}^G(x; x', y'; k_y, k_z) = -\underline{\tilde{J}} \exp(jk_y y')\, \delta(x - x'), \quad (10)$$

$$\underline{\nabla}_t \times \underline{\tilde{\tilde{E}}}^G(x; x', y'; k_y, k_z) + j\omega\mu_0 \underline{\tilde{\tilde{H}}}^G(x; x', y'; k_y, k_z) = \underline{0}, \quad (11)$$

with $\underline{\nabla}^t = (\partial/\partial x, -jk_y, -jk_z)$. In the remainder of this section we will determine the solution of (10), (11) for fixed values k_y and k_z. Furthermore, the y'-dependence of the electric and magnetic fields can easily be seen to equal $\exp(jk_y y')$. Therefore, we will concentrate on the x- and x'-dependence and only these coordinates will appear as arguments of the functions to be determined.

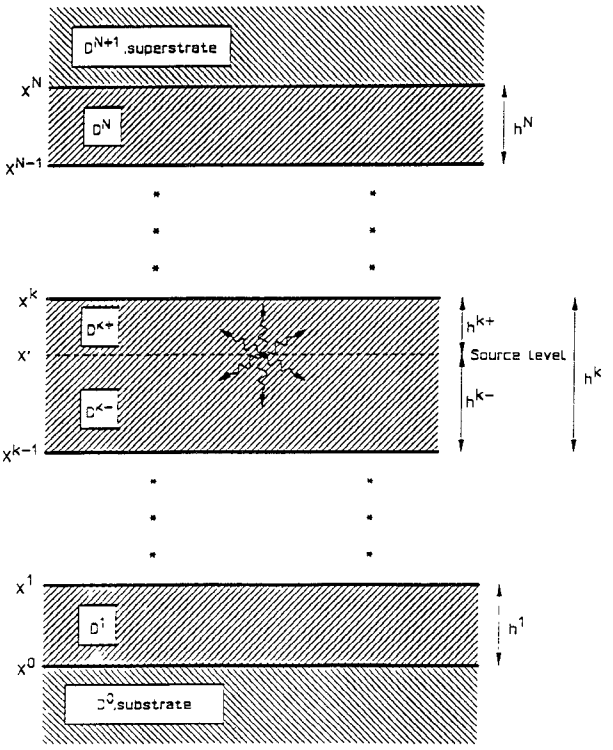

Fig. 2. Electric point source situated in subdomain D^k.

The set of equations (10), (11) consists of 4 first-order ordinary differential equations and two algebraic equations. The algebraic equations are used to eliminate the components $\tilde{\tilde{E}}_1^G$ and $\tilde{\tilde{H}}_1^G$ from the differential equations. The resulting set of ordinary differential equations can be presented in matrix-notation:

$$\frac{\partial \underline{\tilde{\tilde{F}}}^G(x; x')}{\partial x} = A(x) \cdot \underline{\tilde{\tilde{F}}}^G(x; x') + \underline{\mathcal{J}} \cdot \delta(x - x'),$$

$$\underline{\tilde{\tilde{F}}}^G = (Y_0^{1/2} \tilde{\tilde{E}}_2^G, Y_0^{1/2} \tilde{\tilde{E}}_3^G, jZ_0^{1/2} \cdot \tilde{\tilde{H}}_3^G, -jZ_0^{1/2} \tilde{\tilde{H}}_2^G)^T,$$

$$Y_0 = Z_0^{-1} = \frac{\sqrt{\epsilon_0}}{\sqrt{\mu_0}},$$

$$\tilde{\tilde{E}}_1^G = \frac{1}{\omega\epsilon_1} (-k_y \tilde{\tilde{H}}_3^G + k_z \tilde{\tilde{H}}_2^G + j \cdot \tilde{j}_1 \cdot \exp(jk_y y')\, \delta(x - x')),$$

$$\tilde{\tilde{H}}_1^G = \frac{1}{\omega\mu_0} (-k_z \tilde{\tilde{E}}_2^G + k_y \tilde{\tilde{E}}_3^G). \quad (12)$$

The $4 * 4$ matrix $A(x)$ is called the system's matrix. It is x-independent in the interior of each of the subdomains of the embedding. Its components are enumerated in the ap-

pendix. The vectors $\underline{\tilde{F}}^G$ and $\underline{\mathcal{J}}$ are called the field vector and the source vector, respectively, The field vector contains the components of the electromagnetic field which are tangential to the interfaces separating two adjacent subdomains of the embedding. Hence, it is continuous across these interfaces. The components of the electric and magnetic field in the field vector are normalized and are ordered such that the system's matrix consists of only two non-zero blocks on the anti-diagonal (see appendix).

To solve the set of inhomogeneous ordinary differential equations (12) four basic relations are used. These are illuminated in the next subsection.

A. Basic Relations

- General solution within one subdomain.

The set of differential equations (12) is inhomogeneous. In the interior of subdomains D^l, $l \in \{0, \cdots, N+1\}$ however, the field vector satisfies the homogeneous set of ordinary differential equations with x-independent system's matrix $A(x) = A^l$. Using the diagonal decomposition

$$A^l = T^l \cdot \bar{\Lambda}^l \cdot (T^l)^{-1}, \quad \bar{\Lambda}^l_{mn} = 0, \qquad m \neq n, \tag{13}$$

the general solution of the system of homogeneous differential equations equals

$$\underline{\tilde{f}}^G(x; x') = T^l \cdot \exp\left[\bar{\Lambda}^l (x - x^{\text{ref}})\right] \cdot \underline{f}^l(x'), \qquad x^{l-1} \leq x \leq x^l. \tag{14}$$

The vector $\underline{f}^l(x') = (f^l_1(x'), f^l_2(x'), f^l_3(x'), f^l_4 x'))^T$ is called the reference vector subdomain D^l and equals $(T^l)^{-1} \cdot \underline{F}^G(x^{\text{ref}}; x')$ in which $x = x^{\text{ref}}$ is the reference level of subdomain D^l. This reference level equals the lower interface for subdomains above the source-point and equals the upper interface for subdomains underneath the source-point.

For the materials considered in this paper (a more extensive discussion is given in [18]), the eigenvalues of the system's-matrix occur in pairs, having opposite signs (see appendix). This property is reflected in the corresponding eigenvectors:

$$\bar{\Lambda}^l = \text{diag}\,(-\Lambda^l, \Lambda^l), \qquad \Lambda^l = \text{diag}\,(\lambda^l_1, \lambda^l_2), \quad \text{Re}\,\{\lambda^l_1, \lambda^l_2\} \geq 0, \tag{15}$$

$$T^l = \begin{bmatrix} T^l_{11} & -T^l_{11} \\ T^l_{21} & T^l_{21} \end{bmatrix},$$

$$(T^l)^{-1} = \tfrac{1}{2} \begin{bmatrix} (T^l_{11})^{-1} & (T^l_{21})^{-1} \\ -(T^l_{11})^{-1} & (T^l_{21})^{-1} \end{bmatrix}. \tag{16}$$

With (15), (16), an extensive part of the computation of the Green's tensor can be performed analytically if the scattering-matrix formalism is used. This will be shown in the next section.

- Boundary conditions for substrate and superstrate.

For $|x| \to \infty$, the components of the field-vector have to decrease exponentially. This condition is satisfied if (cf. (14), (15))

$$f^0_1(x') = f^0_2(x') = f^{N+1}_3(x') = f^{N+1}_4(x') = 0. \tag{17}$$

- Continuity condition.

The components of the field-vector are continuous across the interfaces $x = x^l$, $l \in \{0, \cdots, N\}$. Hence, the general solution within one subdomain (14) yields

$$\underline{f}^{l+1}(x') = (T^{l+1})^{-1} \cdot T^l \cdot \exp\left[D^l h^l\right] \cdot \underline{f}^l(x'), \qquad l \in \{k+, \cdots, N\}, \text{ and} \tag{18}$$

$$\underline{f}^{l-1}(x') = (T^{l-1})^{-1} \cdot T^l \cdot \exp\left[-D^l h^l\right] \cdot \underline{f}^l(x'), \qquad l \in \{1, \cdots, k-\}. \tag{19}$$

- Connection condition at the source level.

Integration of the inhomogeneous ordinary differential equations (12) over an infinitesimal x-interval containing $x = x'$ yields

$$\underline{f}^{k+}(x') - \underline{f}^{k-}(x') = (T^k)^{-1} \cdot \underline{\mathcal{J}} =: \underline{\tilde{\mathcal{J}}}. \tag{20}$$

In the next subsection, we show how these relations can be used to solve the system of ordinary differential equations (12). The applied formalism is called the scattering-matrix formalism.

B. The Scattering-Matrix Formalism

Using the relations enumerated in the previous section, the different components of the reference vector of one subdomain can be interrelated; the scattering-matrix formalism. For subdomains above the source-point, a downward recursive scheme is used; for subdomains underneath the source-point, an upward recursive scheme is used. The remaining unknown components of the reference vectors are solved by using the connection condition (20).

Before considering the scattering-matrix formalism in detail, two new notations are introduced:

- Let $\underline{v}$ be a vector having four components $\underline{v} = (v_1, v_2, v_3, v_4)^T$, then the vectors $\underline{v}_{12}$ and $\underline{v}_{34}$, having 2 components, are defined as $\underline{v}_{12} = (v_1, v_2)^T$ and $\underline{v}_{34} = (v_3, v_4)^T$ respectively.
- In order to reduce the number of formulae, square brackets are used (see for example (23)). Taking the upper and lower expressions between these brackets successively, two equations result instead of one.

Downward Recursion: The downward transmission-matrix $\mathcal{T}^{d,l}$ and the downward reflection-matrix $\mathcal{R}^{d,l}$ for subdomain D^l, $l \in \{k+, \cdots, N+1\}$, are defined through

$$\underline{f}^{N+1}_{12}(x') = \mathcal{T}^{d,l} \cdot \underline{f}^l_{12}(x'), \qquad \underline{f}^l_{34}(x') = \mathcal{R}^{d,l} \cdot \underline{f}^l_{12}(x'), \quad l \in \{k+, \cdots, N+1\}. \tag{21}$$

The continuity condition (18) and the general solution (14) yields a recursive scheme for the downward reflection-

and transmission-matrix:

$$\begin{aligned}\mathcal{G}^{d,l} &= \mathcal{G}^{d,l+1} \cdot \{B_+^l + B_-^l \cdot \mathcal{R}^{d,l+1}\}^{-1} \\ &\quad \cdot \exp[-\Lambda^l h^l], \\ \mathcal{R}^{d,l} &= \exp[-\Lambda^l h^l] \cdot \{B_-^l + B_+^l \cdot \mathcal{R}^{d,l+1}\} \\ &\quad \cdot \{B_+^l + B_-^l \cdot \mathcal{R}^{d,l+1}\}^{-1} \cdot \exp[-\Lambda^l h^l] \end{aligned} \quad (22)$$

with

$$B_{[\pm]}^l = \tfrac{1}{2} \cdot \left\{ (T_{21}^l)^{-1} \cdot T_{21}^{l+1} + \begin{bmatrix} + \\ - \end{bmatrix} (T_{11}^l)^{-1} \cdot T_{11}^{l+1} \right\}. \quad (23)$$

The recursive scheme is initialized by definition of the downward transmission-matrix and downward reflection-matrix in the cover in accordance with the boundary condition (17) as $\mathcal{G}^{d,N+1} = I$ and $\mathcal{R}^{d,N+1} = 0$ respectively.

Upward Recursion: The upward transmission-matrix $\mathcal{G}^{u,l}$ and the the upward reflection-matrix $\mathcal{R}^{u,l}$ for subdomain D^l, $l \in \{0, \cdots, k-\}$, are defined through

$$\begin{aligned} \underline{f}_{34}^0(x') &= \mathcal{G}^{u,l} \cdot \underline{f}_{34}^l(x'), \\ \underline{f}_{12}^l(x') &= \mathcal{R}^{u,l} \cdot \underline{f}_{34}^l(x'), \qquad l \in \{0, \cdots, k-\}. \end{aligned} \quad (24)$$

The continuity condition (19) and the general solution (14) yield a recursive scheme for the upward reflection- and transmission-matrix:

$$\begin{aligned}\mathcal{G}^{u,l} &= \mathcal{G}^{u,l-1} \cdot \{C_+^l + C_-^l \cdot \mathcal{R}^{u,l-1}\}^{-1} \\ &\quad \cdot \exp[-\Lambda^l h^l], \\ \mathcal{R}^{u,l} &= \exp[-\Lambda^l h^l] \cdot \{C_-^l + C_+^l \cdot \mathcal{R}^{u,l-1}\} \\ &\quad \cdot \{C_+^l + C_-^l \cdot \mathcal{R}^{u,l-1}\}^{-1} \cdot \exp[-\Lambda^l h^l] \end{aligned} \quad (25)$$

with

$$C_{[\pm]}^l = \tfrac{1}{2} \cdot \left\{ (T_{21}^l)^{-1} \cdot T_{21}^{l-1} + \begin{bmatrix} + \\ - \end{bmatrix} (T_{11}^l)^{-1} \cdot T_{11}^{l-1} \right\}. \quad (26)$$

The recursive scheme is initialized by definition of the upward transmission-matrix and upward reflection-matrix in the substrate in accordance with the boundary condition (17) as $\mathcal{G}^{u,0} = I$ and $\mathcal{R}^{u,0} = 0$ respectively.

Interconnecting the Reference Vectors: With the downward recursive outlined above, the reference vectors of subdomains above the point-source are solved as a function of $\underline{f}_{12}^{k+}(x')$. Analogous, the upward recursive scheme is used to solve the reference vectors of subdomains underneath the point-source as a function of the components $\underline{f}_{34}^{k-}(x')$. These last vectors are determined with the connection condition (20). Subsequently, the recursive schemes (22), (25) and the general solution (14) are used to generate the solution of (12) in the entire configuration. For solving the domain-integral equation however, it suffices to determine the Green's tensor for x and x' in the interior of subdomain D^k. The vectors $\underline{f}_{12}^{k+}(x')$ and $\underline{f}_{34}^{k-}(x')$ are x'-dependent only through the scattering matrices of the subdomains $\mathfrak{D}^{k+}$ and $\mathfrak{D}^{k-}$ respectively (all other scattering matrices are x'-independent). This x'-dependence is explicitely known (22), (25). Together with the known x-dependence of the general solution within $\mathfrak{D}^{k+}$ and $\mathfrak{D}^{k-}$, the scattering-matrix formalism allows the Green's tensors to be determined much more explicitely. This will be shown in the next subsection.

C. The Green's Tensor Components

In this subsection, relations are derived explicitly showing the x- and x'-dependence of the field vector $\underline{\tilde{F}}^G(x; x')$ for fixed values k_y and k_z. To this end, the reflection-matrices $\mathcal{R}^d$ and $\mathcal{R}^u$ are introduced as being the downward and upward reflection-matrix corresponding to the point-source situated *at the center* of subdomain $\mathfrak{D}^k$; $x' = 0$. The recursive schemes (22), (25) yield expressions for the reflection-matrices, for points x' in $\mathfrak{D}^k$ different from $x' = 0$ ($\Lambda := \Lambda^k$);

$$\begin{aligned} \mathcal{R}^{d,k+}(x') &= \exp[\Lambda x'] \cdot \mathcal{R}^d \cdot \exp[\Lambda x'], \\ \mathcal{R}^{u,k-}(x') &= \exp[-\Lambda x'] \cdot \mathcal{R}^u \cdot \exp[-\Lambda x']. \end{aligned} \quad (27)$$

Together with the definition of the reflection-matrices, these expressions are used in the connection condition to give

$$\begin{aligned} \underline{f}_{[34]}^{k+[12]}(x') &= \exp\left[\begin{bmatrix} - \\ + \end{bmatrix} \Lambda x'\right] \\ &\quad \cdot \begin{bmatrix} I \\ \mathcal{R}^d \end{bmatrix} \cdot \{I - \mathcal{R}^u \cdot \mathcal{R}^d\}^{-1} \cdot \exp[\Lambda x'] \\ &\quad \cdot \underline{\mathcal{J}}_{12} - \exp\left[\begin{bmatrix} - \\ + \end{bmatrix} \Lambda x'\right] \cdot \begin{bmatrix} I \\ \mathcal{R}^d \end{bmatrix} \\ &\quad \cdot \{I - \mathcal{R}^u \cdot \mathcal{R}^d\}^{-1} \cdot \mathcal{R}^u \\ &\quad \cdot \exp[-\Lambda x'] \cdot \underline{\mathcal{J}}_{34}, \\ \underline{f}_{[34]}^{k-[12]}(x') &= \exp\left[\begin{bmatrix} - \\ + \end{bmatrix} \Lambda x'\right] \cdot \begin{bmatrix} \mathcal{R}^u \\ I \end{bmatrix} \\ &\quad \cdot \{I - \mathcal{R}^d \cdot \mathcal{R}^u\}^{-1} \cdot \mathcal{R}^d \\ &\quad \cdot \exp[\Lambda x'] \cdot \underline{\mathcal{J}}_{12} \\ &\quad - \exp\left[\begin{bmatrix} - \\ + \end{bmatrix} \Lambda x'\right] \cdot \begin{bmatrix} \mathcal{R}^u \\ I \end{bmatrix} \\ &\quad \cdot \{I - \mathcal{R}^d \cdot \mathcal{R}^u\}^{-1} \cdot \exp[-\Lambda x'] \cdot \underline{\mathcal{J}}_{34}. \end{aligned} \quad (28)$$

Substitution in the general solution within subdomain $\mathfrak{D}^k$ (14) reveals the explicit x- and x'-dependence of the field-

vector $\tilde{\underline{\tilde{F}}}^G(x; x')$;

$$\tilde{\underline{\tilde{F}}}^G_{\begin{bmatrix}12\\34\end{bmatrix}}(x; x') = \tfrac{1}{2}T^k_{\begin{bmatrix}11\\21\end{bmatrix}} \cdot \left\{ \exp[-\Lambda x] + \begin{bmatrix}-\\+\end{bmatrix} \exp[\Lambda x] \cdot \mathfrak{R}^d \right\} \cdot \{I - \mathfrak{R}^d\}^{-1} \cdot \langle \{\exp[\Lambda x'] + \mathfrak{R}^u \cdot \exp[-\Lambda x']\} \cdot (T^k_{11})^{-1} \cdot \underline{\mathfrak{J}}_{12} + \{\exp[\Lambda x'] - \mathfrak{R}^u \cdot \exp[-\Lambda x']\} \cdot (T^k_{21})^{-1} \cdot \underline{\mathfrak{J}}_{34} \rangle, \quad x^{k-1} < x' < x < x^k, \tag{29}$$

$$\tilde{\underline{\tilde{F}}}^G_{\begin{bmatrix}12\\34\end{bmatrix}}(x; x') = \tfrac{1}{2}T^k_{\begin{bmatrix}11\\21\end{bmatrix}} \cdot \left\{ \begin{bmatrix}-\\+\end{bmatrix} \exp[\Lambda x] + \exp[-\Lambda x] \right\} \cdot \mathfrak{R}^u \cdot \{I - \mathfrak{R}^d \cdot \mathfrak{R}^u\}^{-1} \cdot \langle \{\exp[-\Lambda x'] + \mathfrak{R}^d \cdot \exp[\Lambda x']\} \cdot (T^k_{11})^{-1} \cdot \underline{\mathfrak{J}}_{12} - \{\exp[-\Lambda x'] - \mathfrak{R}^d \cdot \exp[\Lambda x']\} \cdot (T^k_{21})^{-1} \cdot \underline{\mathfrak{J}}_{34} \rangle, \quad x^{k-1} < x < x' < x^k. \tag{30}$$

For $\underline{J} = (\tilde{j}_1, \tilde{j}_2, \tilde{j}_3)$ equal to the i-th unit vector ($i = 1, 2, 3$), the components of $\tilde{\underline{\tilde{F}}}^G_{12}$ yield the Fourier-transformed electric Green's tensor components $\tilde{\tilde{G}}^{EE}_{2i}$ and $\tilde{\tilde{G}}^{EE}_{3i}$. The component $\tilde{\tilde{G}}^{EE}_{1i}$ follows from the linear relations in (12). The electric Green's tensor in the spatial (x, y)-domain $\underline{\underline{\tilde{G}}}^{EE}$, is obtained through inverse Fourier-transformation with respect to k_y. Similarly, the magnetic Green's tensor is derived from the components of $\tilde{\underline{\tilde{F}}}^G_{34}$.

IV. Numerical Implementation

In order to find the nontrivial solutions of the domain-integral equation, the method of moments is applied [20]. The cross-section of the channel-waveguide D^w is divided into L rectangular subdomains S^l, $l \in \{1, \cdots, L\}$. Rectangle functions are used as expansion functions, which take the value 1 within S^l and vanish outside S^l. For the weighting functions, Dirac functions are used (point-matching). Assuming that the electric field strength in S^l is constant and equal to the actual electric field strength $\tilde{\underline{E}}^l$ in the barycenter (x^l, y^l) of S^l, the method of moments yields

$$\tilde{\underline{E}}^k \approx \frac{j\omega}{2\pi} \sum_{l=1}^{L} \iint_{S^l} \int_{-\infty}^{\infty} \underline{\underline{\tilde{G}}}^{EE}(x^k; x', y', k_y, k_z) \cdot \exp(-jk_y y^k)\, dk_y\, dx'\, dy' \{\underline{\underline{\epsilon}}^w - \underline{\underline{\epsilon}}^b\} \tilde{\underline{E}}^l, \quad k \in \{1, \cdots, L\}. \tag{31}$$

This is a system of $3 * L$ linear algebraic equations for the $3 * L$ unknown components of the electic field strength; $\tilde{E}^k_i$, $k \in \{1, \cdots, L\}$, $i \in \{1, 2, 3\}$. A numerical implementation has been made for the important class of uniaxially anisotropic materials having optic axis perpendicular to the interface of two adjacent subdomains of the embedding. In the appendix, the components of the decomposition matrix T^l and the corresponding diagonal-matrix Λ^l are listed. For these materials, the reflection matrices $\mathfrak{R}^d$ and $\mathfrak{R}^u$ are diagonal matrices. Therefore, the computation of the components of the Green's tensor using (29), (30) can be performed using scalar instead of matrix arithmetic. Hence, CPU-times are reduced considerably with respect to full matrix methods (e.g. [17]).

In determining the contribution of subdomain S^l, the order of spatial integration over S^l and inverse Fourier-transformation with respect to k_y is interchanged; first the relations (29), (30) are integrated over S^l, next the inverse Fourier transformation is evaluated. For the inverse Fourier transformation, special care has to be taken of the spectral plane singularities in the complex k_y plane: for $k_z^2 + k_y^2 = \beta_{SWM}$, β_{SWM} being the propagation constant of a surface wave mode of the layered embedding, the components of the Green's tensors are singular. Therefore, if k_z is larger than the largest β_{SWM}, no problems in the inverse Fourier transformation over the real axis occur. If k_z is less than the largest β_{SWM}, the integration path of the inverse Fourier transformation is deformed into the first and third quadrant of the complex k_y plane around the surface wave poles.

The interchanging of the order of integrations accomplishes the convergence of the inverse Fourier-transformation ([21], Problem 2.31). The spatial integration over the subdomains S^l can easily be performed analytically. The inverse Fourier-transformation for the non-exponentially decaying part of the integrand is also performed analytically. The inverse Fourier-transformation for the remaining exponentially decaying part of the integrand is performed using a Fast Fourier Transformation algorithm.

Subsequently, the system of linear algebraic equations is solved by searching for those values of $k_z = \beta^m$ for which a nontrivial solution exists. Once these eigenvalues β^m have been determined, the accompanying eigenvector is calculated. Obviously, the eigenvalue β^m corresponds to a propagation constant of a propagating guided wave mode, and the eigenvector to its electric field distribution within the waveguide $\mathfrak{D}^w$.

V. Numerical Results

To illustrate the theory developed in the previous sections, it is used to investigate the influence of neglecting the anisotropic character of the embedding of a polymeric single-rib waveguide. To do so, the propagation constants of the fundamental modes of the waveguiding structure are calculated. Although all modes are hybrid (none of the field components equals zero), the fundamental modes are denoted as Transverse Electric (TE_{00}, $\tilde{\tilde{E}}_2$ is the dominant electric field component) and Transverse Magnetic (TM_{00}, $\tilde{\tilde{E}}_1$ is the dominant electric field component) re-

spectively. The waveguiding structure consists of an uniaxially anisotropic ridge waveguide, embedded in a uniaxially anistotropic stratified medium. This waveguide has been developed within the framework of the project RACE 1019 (Research on Advanced Communication Technologies in Europe). A domain-integral equation analysis of a similar waveguide has been presented in [17], where the waveguiding structure was assumed to be isotropic.

The embedding consists of a glass substrate (refractive index 1.5) on which three polymeric layers are deposited (Fig. 3); two polyurethane buffer layers of thickness 2.0 μm and a central guiding layer of thickeness 2.5 μm. The buffer layers are isotropic (refractive index 1.523). The central guiding layer consists of an uniformly poled electro-optical polymer. The poled polymer is uniaxially anisotropic, the optical axis being normal to the interfaces of the embedding; $n^e = \sqrt{\epsilon_1} = 1.606$, $n^o = \sqrt{\epsilon_2} = \sqrt{\epsilon_3} = 1.576$. In the electro-optical polymer, a rib with a width $w = 5.0$ μm is photochemically induced, using ultra violet exposure [22]. The rib height r depends on the exposure-time. Due to the ultra-violet exposure, the refractive indices of the anisotropic poled polymers decrease to the isotropic value $n^e = n^o = 1.556$. For this configuration, the propagation constants of the fundamental modes TE_{00} and TM_{00} are determined as a function of r. The waveguide is operated at the free-space wavelength $\lambda_0 = 1.335$ μm. The numerical results are compared with results obtained by replacing the embedding of the waveguiding structure with a corresponding isotropic one. For TE modes, the dominant electric field component is parallel to the interfaces. Therefore, the corresponding isotropic embedding is obtained by replacing the uniaxially permittivity tensor by the isotropic permittivity $\epsilon = (n^o)^2 = 1.576^2$. For TM modes, the dominant electric field component is normal to the interfaces. Therefore, the corresponding isotropic embedding is obtained by replacing the uniaxially permittivity tensor by the isotropic permittivity $\epsilon = (n^e)^2 = 1.606^2$ (Fig. 4). The waveguide itself remains uniaxial.

To increase the accuracy of the results, the channel waveguide has been divided in Q subdomains in the x-direction and P subdomains in the y-direction ($L = P * Q$), for ranging values of P and Q. For $r = 1.5$ micron and $P = 4 * Q + 4$, Fig. 5 gives the calculated values of the effective refractive index of the fundamental TM mode for both the isotropic and the uniaxial case as a function of $1/L$. By extrapolation of this function for $1/L \to 0$, extremely accurate results for the effective refractive index are obtained.

Table I and Table II show the effective refractive indices $N_{\text{eff}} = \beta/k_0$ as a function of r for the TE_{00} and TM_{00} mode respectively, for both the uniaxially waveguide and its isotropic counterpart.

The numerical results show that approximating the uniaxially waveguiding structure by its isotropic counterpart, leads to only small errors. The errors for TM-modes are larger than for TE-modes. This is due to the fact that for TE modes the normal component of the electric field is negligible. Therefore, the replacement of the extra-ordinary component of the permittivity tensor by the ordinary component is of little influence. For TM modes how-

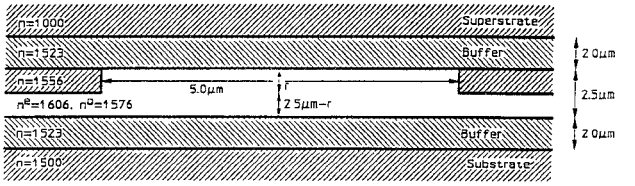

Fig. 3. Polymeric rib waveguide developed within RACE 1019.

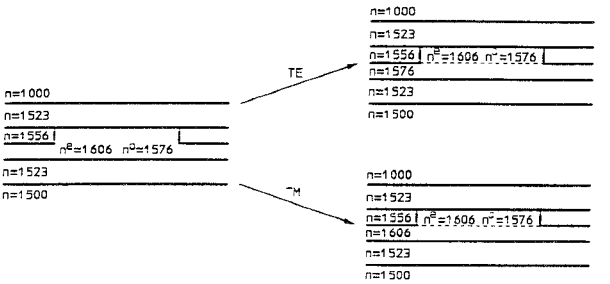

Fig. 4. Replacement of the uniaxial embedding by a corresponding isotropic embedding.

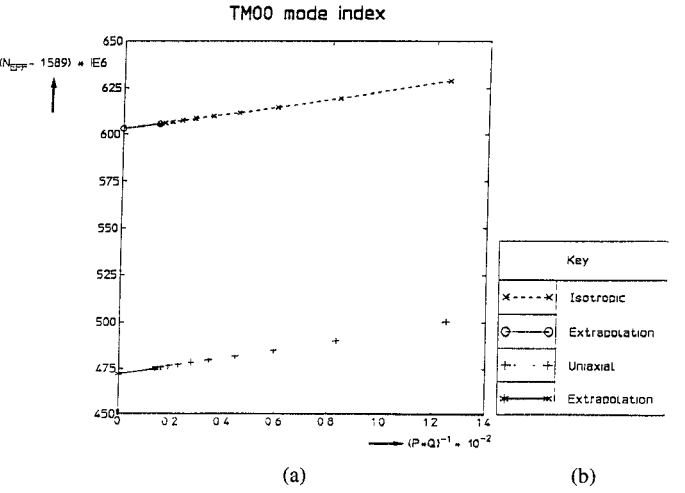

Fig. 5. The calculated effective refractive index for the fundamental TM modes as a function of the number L: (a) isotropic embedding, (b) uniaxial embedding.

TABLE I
THE NORMALIZED EFFECTIVE REFRACTIVE INDEX $(N_{\text{eff}} - 1.56) * 1E5$ FOR THE FUNDAMENTAL TRANSVERSE ELECTRIC MODE TE_{00} AS A FUNCTION OF THE RIB-HEIGHT r

r	Isotropic	Uniaxial
0.5	389	389
1.0	303	303
1.5	240	240
2.0	203	203
2.5	188	188

TABLE II
THE NORMALIZED EFFECTIVE REFRACTIVE INDEX ($N_{\text{eff}} - 1.58$) * 1E5 FOR THE FUNDAMENTAL TRANSVERSE MAGNETIC MODE TM_{00} AS A FUNCTION OF THE RIB-HEIGHT r

r	Isotropic	Uniaxial
0.5	1133	1114
1.0	1025	1011
1.5	960	947
2.0	925	915
2.5	903	903

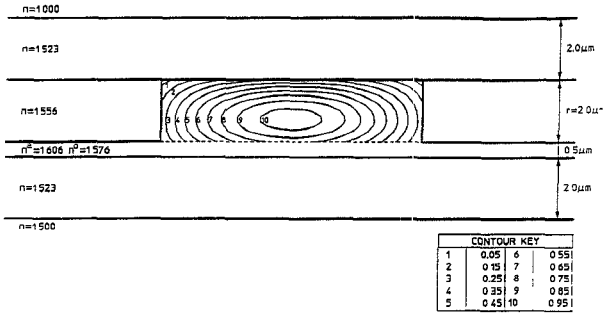

Fig. 6. The electric field intensity for the TM_{00}-mode inside the channel waveguide ($r = 2.0$ micron).

ever, the component of the electric field parallel to the interfaces can not be neglected, even though it is an order of magnitude smaller than the normal component. Hence, replacing the ordinary component of the permittivity tensor by the extra-ordinary component does have a certain amount of influence on the effective refractive indices.

Once the eigenvalues $k_z = \beta^m$ have been determined, for which the system of linear equations (31) have a non-trivial solution, the corresponding null-vector yields the electric field inside the channel waveguide. In Fig. 6 the intensity of the electric field of the TM_{00}-mode inside the channel waveguide is shown for the case of the uniaxial embedding and $r = 2.0$ micron. Subsequently, the electric and magnetic field everywhere in the configuration can be found using the integral representation (4), (5).

VI. CONCLUSIONS

A domain-integral equation method has been presented for determining both propagation constants and modal field-distributions of guided surface wave modes of optical waveguides, embedded in a multi-layered medium. Both the waveguide and its embedding may be anisotropic. Furthermore, the waveguide may be inhomogeneous. A scattering-matrix formalism is presented, which efficiently evaluates the kernel of the integral equations. The integral equation method is successfully applied in the numerical computation of the propagation constants of a rib waveguide bleached in an electro-optical polymer, having both an anisotropic rib and anisotropic embedding.

APPENDIX

For materials of the embedding having a permittivity tensor that satisfies

$$\underline{\underline{\epsilon}}^{\,l} = \epsilon_0 \operatorname{diag}(\epsilon_1^{r,l}, \epsilon_2^{r,l}, \epsilon_3^{r,l}),$$
$$l \in \{0, \cdots, N+1\}, \tag{32}$$

the $4 * 4$ system's matrix A^l equals

$$A^l = \begin{bmatrix} 0 & A_{12}^l \\ A_{21}^l & 0 \end{bmatrix} \tag{33}$$

with

$$A_{12}^l = \frac{k_0}{\epsilon_1^{r,l}} \cdot \begin{bmatrix} N_y^2 - \epsilon_1^{r,l} & N_y N_z \\ N_y N_z & N_z^2 - \epsilon_1^{r,l} \end{bmatrix},$$
$$A_{21}^l = k_0 \cdot \begin{bmatrix} -N_z^2 + \epsilon_2^{r,l} & N_y N_z \\ N_y N_z & -N_y^2 + \epsilon_3^{r,l} \end{bmatrix},$$
$$N_{y,z} = k_{y,z}/k_0, \quad k_0 = \omega\sqrt{\epsilon_0 \mu_0}. \tag{34}$$

Furthermore, for a point source situated in subdomain D^k the source vector equals

$$\underline{\mathcal{J}} = Z_0^{1/2} \cdot \begin{bmatrix} N_y \cdot \tilde{j}_1/\epsilon_1^{r,k} \\ N_z \cdot \tilde{j}_1/\epsilon_1^{r,k} \\ -j \cdot \tilde{j}_2 \\ -j \cdot \tilde{j}_3 \end{bmatrix} \cdot \exp(jk_y y'). \tag{35}$$

The characteristic polynomial $p(\lambda) = \det(A^l - \lambda I)$ is of degree two in λ^2. Hence, the eigenvalues of A^l appear in pairs, having opposite signs. Furthermore, $\underline{v} = (v_1, v_2, v_3, v_4)^T$ being the eigenvector corresponding to the eigenvalue λ, the eigenvector corresponding to the eigenvalue $-\lambda$ equals $\underline{v}' = (-v_1, -v_2, v_3, v_4)^T$. This results in the diagonal decomposition according to (15), (16).

For uniaxial materials with optic axis perpendicular to the interfaces, the permittivity tensor satisfies $\epsilon_2^{r,l} = \epsilon_3^{r,l}$, and the diagonal decomposition of the system's matrix is given by

$$\lambda_1^l = k_0 \cdot \sqrt{\frac{\epsilon_2^{r,l}}{\epsilon_1^{r,l}}} \cdot \sqrt{N_y^2 + N_z^2 - \epsilon_1^{r,l}},$$
$$\lambda_2^l = k_0 \cdot \sqrt{N_y^2 + N_z^2 - \epsilon_2^{r,l}},$$
$$T_{11}^l = \begin{bmatrix} -N_y \cdot \sqrt{N_y^2 + N_z^2 - \epsilon_1^{r,l}} & N_z \\ -N_z\sqrt{N_y^2 + N_z^2 - \epsilon_1^{r,l}} & -N_y \end{bmatrix},$$
$$T_{21}^l = \begin{bmatrix} N_y \cdot \sqrt{\epsilon_1^{r,l}\epsilon_2^{r,l}} & N_z \cdot \sqrt{N_y^2 + N_z^2 - \epsilon_2^{r,l}} \\ N_z \cdot \sqrt{\epsilon_1^{r,l}\epsilon_2^{r,l}} & -N_y \cdot \sqrt{N_y^2 + N_z^2 - \epsilon_2^{r,l}} \end{bmatrix}. \tag{36}$$

REFERENCES

[1] J. J. G. M. van der Tol and N. H. G. Baken, "Correction to effective index method for rectangular dielectric waveguides," *Electron. Lett.*, vol. 24, no. 4, pp. 207–208, Feb. 1988.

[2] R. M. Knox and P. P. Toulios, "Integrated circuits for millimeter through optical frequency range," in *Proc. MRI Symp. Subm. Waves*, Apr. 1970, pp. 497–516.
[3] M. S. Stern, "Semivectorial polarised H field solutions for dielectric waveguides with arbitrary index profiles," *Proc. Inst. Elec. Eng.*, vol. 125, pt. J, no. 5, pp. 333–338, Oct. 1988.
[4] ——, "Semivectorial polarised finite difference method for optical waveguides with arbitrary indix profiles," *Proc. Inst. Elec. Eng.*, vol. 135, pt. J, no. 1, pp. 56–63, Feb. 1988.
[5] P. L. N. Mabaya, P. E. Lagasse, and P. Vandenbulcke, "Finite element analysis of optical waveguides," *IEEE Trans. Microwave Theory Tech.*, vol. 29, pp. 600–605, June 1981.
[6] C. Yeh, S. B. Dong, and W. Oliver, "Arbitrarily shaped inhomogeneous optical fiber or intergrated optical waveguides," *J. Appl. Phys.*, vol. 46, pp. 2125–2129, May 1975.
[7] B. Rahman and J. Davies, "Finite-element analysis of optical and microwave waveguide problems," *IEEE Trans. Microwave Theory and Tech.*, vol. 32, pp. 20–28, Jan. 1984.
[8] J. E. Goell, "A circular-harmonic computer analysis of rectangular dielectric waveguides," *Bell Syst. Tech. J.*, vol. 48, pp. 2133–2160, Sept. 1969.
[9] P. G. L. Eyges, P. Gianino, and P. Wintersteiner, "Modes of dielectric waveguides of arbitrary cross sectional shape," *J. Opt. Soc. Am.*, vol. 69, pp. 1226–1235, Nov. 1979.
[10] N. Morita, "A method extending the boundary conditions for analyzing guided modes of dielectric waveguides of arbitrary cross sectional shape," *IEEE Trans. Microwave Theory Tech.*, vol. 30, pp. 6–12, Jan. 1982.
[11] C. C. Su, "A surface integral equations method for homogeneous optical fibers and coupled image lines of arbitrary cross sections," *IEEE Trans. Microwave Theory Tech.*, vol. 33, no. 11, pp. 1114–1119, Nov. 1985.
[12] ——, "A combined method for dielectric waveguides using the finite-element technique and the surface integral equations method," *IEEE Trans. Microwave Theory Tech.*, vol. 34, no. 11, pp. 1140–1145, Nov. 1986.
[13] C. Pichot, "Exact numerical solution for the diffused channel waveguide," *Optics Comm.*, vol. 41, no. 3, pp. 169–173, Apr. 1982.
[14] J. S. Bagby, D. N. Nyquist, and B. C. Drachman, "Integral formulation for analysis of integrated dielectric waveguides," *IEEE Trans. Microwave Theory Tech.*, vol. MTT-33, no. 10, pp. 906–915, Oct. 1985.
[15] N. H. G. Baken, M. B. J. Diemeer, J. M. van Splunter, and H. Blok, "Computational modeling of diffused channel waveguides using a domain-integral equation," *J. Lightwave Tech.*, vol. 8, no. 4, pp. 576–586, 1990.
[16] P. Cottis and N. Uzunoglu, "Integral equation approach for the analysis of anisotropic channel waveguides," *J. Opt. Soc. Am A*, vol. 8, no. 4, pp. 608–614, Apr. 1991.
[17] E. W. Kolk, N. H. G. Baken, and H. Blok, "Domain-integral equation analysis of integrated-optical channel and ridge waveguides in stratified media," *IEEE Trans. Microwave Theory Tech.*, vol. 38, no. 1, pp. 78–85, Jan. 1990.
[18] N. H. G. Baken, "Computational modeling of integrated-optical waveguides," Ph.D. dissertation, Drukkerij Plantijn, Rotterdam, 1990.
[19] T. Sphicopoulos, V. Teodoridis, and F. E. Gardiol, "Dyadic Green function for the electromagnetic field in multilayered isotropic media: an operator approach," *Proc. Inst. Elect. Eng.*, vol. 132, pt. H, no. 5, pp. 329–334, Aug. 1985.
[20] R. F. Harrington, "The method of moments in electromagnetics," *J. Electromagnetic Waves and Applications*, vol. 1, no. 3, pp. 181–200, 1987.
[21] R. Collin, Ed., *Field theory of Guided Waves*, 2nd ed. IEEE Press, New York: 1991.
[22] M. Diemeer *et al.*, "Photoinduced channel waveguide formation in nonlinear optical polymers," *Electron. Lett.*, vol. 26, pp. 379–380, Sept. 1989.

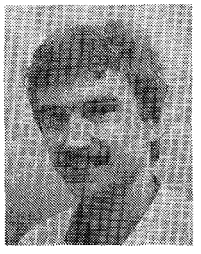

Harrie J. M. Bastiaansen was born in Tilburg, The Netherlands, on May 10, 1965. He received his M.Sc. degree in mathematics, cum laude, from the Eindhoven University of Techonology in 1988, having specialized in the mechanics of rigid bodies.

In 1989, he became a Researcher at the PTT Neher Laboratories, Leidschendam, the Netherlands. Initially, his interest was in the guided wave characteristics of straight channel waveguides. At present, he is working on the Ph.D. thesis on the subject of guided wave optics in bent channel waveguides.

Nico H. G. Baken was born in Eindhoven, The Netherlands, on July 2, 1955. He graduated in mathematics from the Eindhoven University of Technology, where he received, cum laude, his M.Sc. degree in 1981.

In 1982, he joined the PTT Research Neher Laboratories, Leidschendam, The Netherlands. His work involved the calculation of electromagnetic fields in straight channel waveguides, for which he received the Ph.D. degree in 1990. At present, he is with the strategy group of the Dutch PTT, in which he is working on the introduction of the optical fibre in the Dutch telecommunications network.

Hans Blok was born in Rotterdam, The Netherlands, on April 14, 1935. He received a degree in electrical engineering from the Polytechnical School of Rotterdam in 1956. He then received the B.Sc. and M.Sc. degrees in electrical engineering and the Ph.D. degree in technical sciences, all form the Delft Univesity of Technology, in 1961, 1963, and 1970 respectively.

Since 1968, he has been a member of the Scientific Staff of the Laboratory of Electromagnetic Research at the Delft University of Technology. During these years, he has carried out research and lectured in the areas of signal processing, wave propagation, and scattering problems. During the academic year 1970–1971, he was a Royal Society Research Fellow in the Department of Electronics of the University of Southampton, U.K., where he was involved in experimental and theoretical research on lasers and nonlinear optics. In 1972 he was appointed Associate Professor at the Delft University of Technology, and in 1980 he was named Professor. From 1980 to 1982 he was Dean of the Faculty of Electrical Engineering. During the academic year 1983–1984 he was visiting scientist at Schlumberger-Doll Research, Ridgefield, CT. At present, his main interest is in guided wave optics and inverse scattering problems.